

ANALYSIS OF THE EFFECT OF SPRAY MODE ON COATING POROSITY AND HARDNESS WHEN SPRAYING PRESS SCREWS BY THE HIGH VELOCITY OXY FUEL METHOD

Tuan-Linh Nguyen✉

Department of Mechanical Engineering¹
nguyentuanlinh@hau.edu.vn

Hong Tien Nguyen

Department of Mechanical Engineering¹

Van Thien Nguyen

Department of Personel and Administration¹

Duc Duong Khuat

Department of Mechanical Engineering¹

¹*Hanoi University of Industry*

298 Cau Dien str., Bac Tu Liem dist., Hanoi, Vietnam, 10000

✉Corresponding author

Abstract

Porosity and coating hardness are two very important properties of the coating. In order to achieve low coating porosity and high hardness, a suitable spray mode is desired. In the particular application for press screws with the complex surface, a suitable spray mode plays a significant role in the formation of the coating properties. This paper employs the Taguchi experimental design method combined with ANOVA analysis to evaluate the impact of the spray mode on the porosity and hardness of the coating while spraying the screw surface using the High Velocity Oxy Fuel (HVOF) method. The injection material used is WC HMSP1060-00 +60 % 4070, with its main components being Nickel and Carbide Wolfram. And the press screw material is 1045 steel. The impactful parameters of the spray mode investigated and tested are the flow rate of spray (F) with a range varying from 25 g/min to 35 g/min, spray distance (D) with a range of values varying from 0.25 m to 0.35 m, and an oxygen/propane ratio (R) from 4 to 6. The analysis shows that the spray mode significantly affects the coating properties, and a suitable set of spray parameters is found to achieve low coating porosity and high coating hardness. The spray mode with the lowest porosity is achieved at a spray rate (F) of 35 g/min, a spray distance (D) of 0.3 m, and an oxygen/propane ratio (R) of 6. The interactions between D and R , as well as between F and D , are statistically significant, influencing each other's effects on porosity. However, the interaction between F and R is relatively low, indicating that changes in one parameter have less impact on porosity when the other parameter is varied. Similarly, for the highest coating hardness, the optimal spray mode includes an F of 35 g/min, D of 0.25 m, and R of 6. There is a significant interaction between F and D , while the interaction between F and R is relatively low. Notably, there is no interaction between F and R .

Keywords: spray mode, coating porosity, coating hardness, HVOF method, press screw.

DOI: 10.21303/2461-4262.2023.003161

1. Introduction

The HVOF (High Velocity Oxygen Fuel) method is a high-speed injection process that uses oxygen and fuel with injection speeds that can reach 1000 to 1500 m/sec. The structure of HVOF coating is typically studied and determined using a scanning electron microscope or optical microscope. The coating has a layered structure with properties, composition, and structure that differs from the original material. The coating is made up of metal sheets that range in size from 0.1 to 0.2 mm with a thickness of 0.005 to 0.01 mm stacked on top of each other [1]. Each metal plate undergoes varying degrees of deformation and is separated by a thin layer of oxide with a thickness of approximately 0.001 mm.

The HVOF coating structure is characterized by a set of specific parameters, including porosity, oxide film, particle geometry, binder, residual stress, non-melting particles, interlayer, impurities, and cracks. The complex structure of HVOF coatings is due to the high temperature, high pressure, and strong mechanical impact under which the coating is formed.

Porosity is one of the most impactful parameters in HVOF coatings. Coating porosity is defined as the percentage by volume of voids per volume of the coating, and it typically ranges between 0.1 and 15 % for thermal spray coatings. However, evaluating porosity through the volumetric method is challenging. As a result, technical standards organizations have introduced a method for evaluating coating porosity using the metallographic image of the coating cross-section in the thickness direction. Porosity is calculated as the percentage of the area occupied by voids in the image relative to the total area of the metallographic image under consideration. The magnification ratio of the image is typically between 100 and 500 times. Measurement accuracy can be ensured by performing porosity determination on multiple images at different locations using specialized calculation software. Porosity greatly affects the workability of the coating, which is formed by the interactions between the spray particles and the substrate surface, as well as between the spray particles during the spraying process. Therefore, porosity is a component that always exists in thermal coatings, and its content depends on process factors, technological parameters, or spraying methods. Granules that do not melt and those that cool during spraying produce high porosity during coating cooling. Porosity is also affected by the energy acting on the particles through particle velocity and temperature, local stress shrinkage of the particles when cooled, injection angle, temperature, particle size, and surface treatment process before spraying.

Numerous studies have shown that the HVOF thermal spray process provides coatings with the lowest porosity of the commonly used thermal spray processes. This is a direct result of the high particle velocity and low temperature flame [2]. Some studies [3, 4] show that the process evolution of particles during spraying has an important influence on the microstructure and phase composition of the formed coating. The factors have not only a partial effect but also a combined interaction under specific conditions. Porosity reflects the basic properties of the coating, and usually, the lower the porosity is, the better the coating formation and quality properties are. If the porosity is too high, it will reduce strength, abrasion resistance, and corrosiveness. Therefore, it is necessary to determine the spray parameter range for coatings with high properties, including low porosity.

Hardness is a crucial property that significantly affects the wear resistance of the coating, in addition to porosity. Therefore, to enhance the coating's hardness, the spray method is an important factor, apart from the material factor. The HVOF coating exhibits a heterogeneous structure comprising coating, oxide, and pore materials. Normally, the hardness of the coating is a characteristic of the coating material properties, and it depends on the hardness of the sprayed material. However, during thermal spraying, the hardness of the coating changes due to the influence of the heat source characteristics, particle speed, and spray process characteristics. The spray particles undergo deformation and forging during the coating formation process, leading to an increased density and durability of the coating, thereby improving the coating hardness. The HVOF spray method, which employs high-speed spray particles and temperature. It is differentiated with other methods by facilitating increased strength and hardness of the material [5].

2. Materials and methods

2. 1. The test sample

The test sample is fabricated using 1045 steel, a grade of steel which is commonly utilized in mechanical structures and is ideal for manufacturing parts with helical shape like press screws. **Table 1** [6] illustrates the chemical composition of 1045 steel.

Table 1

Chemical composition of 1045 steel

| Steel mark | C(%) min-max | Si(%) min-max | Mn(%) min-max | P(%) max | S(%) max | Cr(%) min-max |
|------------|--------------|---------------|---------------|----------|----------|---------------|
| 1045 | 0.42÷0.50 | 0.15÷0.35 | 0.50÷0.80 | 0.025 | 0.025 | 0.20÷0.40 |

After cutting the press screw, the resulting sample is mounted onto the meter for testing purposes. To prepare the sample for measurement, it is polished and coated with the desired surface material. The shape and dimensions of the experimental sample are depicted in **Fig. 1**.



Fig. 1. The shape of the sample test

2. 2. HVOF spray equipment and materials

The injection process is controlled by using the HVOF spray device with the HP-2700 M spray gun to match the profile of the press screw. The HVOF spray device is shown in **Fig. 2**.



Fig. 2. HVOF spray equipment

Main parameters of the HVOF injection equipment system: Spray flow ($F = 15\div 50$ g/min), spray distance ($D = 0.15\div 0.5$ m), oxygen/propane ratio ($R = 2\div 7$), powder feeding accuracy (0.1 g/rev), the required control pressure from 0 to 11 Bar, adjustable pressure within ± 0.1 Bar.

Using WC spray powder HMSP1060-00+60 % 4070 containing Nickel element combined with Wolfram carbide has good friction and wear resistance, suitable for creating high wear-resistant coatings for press screws when the press screws work under relatively high pressure and temperature conditions. The chemical composition of this spray powder is shown in **Table 2**.

Table 2

Chemical composition of spray powder WC HMSP1060-00+60 % 4070

| Element | C | Ni | Fe | Cr | Si | B | WC |
|-----------|------|-------|------|------|----|-----|-------|
| Ratio (%) | 2.96 | 27.59 | 1.85 | 6.45 | 2 | 1.4 | 57.75 |

The physical properties of WC and Ni are shown in **Table 3**.

Table 3

The physical properties of WC and Ni

| No. | Physical properties | WC | Ni |
|-----|--------------------------------------|-----------|------|
| 1 | Melting temperature (°C) | 2785–2830 | 1455 |
| 2 | Module Young (GPa) | 530–700 | 200 |
| 3 | Specific weight (g/cm ³) | 15.6 | 8.9 |

2. 3. Method of measuring porosity and coating hardness

The test samples used for measurement include nine samples with nine different spray modes. Nine different spray modes are created by varying the injection flow rate (F) with three levels: 25, 30, and 35 g/min. Changing the spray distance (D) with three levels: 0.2, 0.25, and 0.3 m. Changing the oxygen/propane ratio (R) to three levels: 4–6.

The coating porosity was measured on a Leica optical microscope. Magnification of the microscope ranges from 5 to 300 times. The Leica optical microscope image is shown in **Fig. 3**.

Coating hardness is measured by diamond piercing in the direction perpendicular to the coating surface, the coating hardness value is based on the depth and width of the indentation obtained [7]. The ISOSCAN HV2 AC hardness tester used to measure is shown in **Fig. 4**.

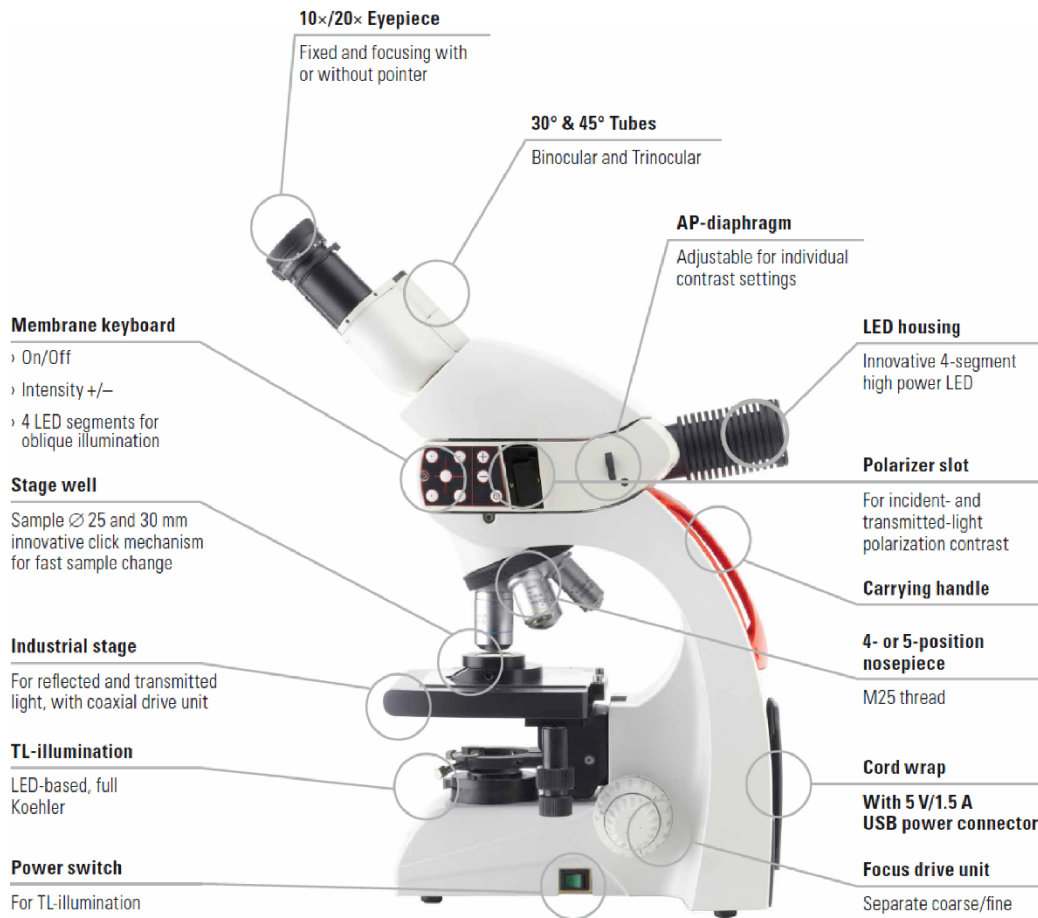


Fig. 3. Optical microscope LEICA DM750 M



Fig. 4. Hardness tester ISOSCAN HV2 AC

3. Results and discussion

3. 1. Analysis results of coating porosity

The coating structure is characterized by many parameters but porosity (Po) is an important parameter. **Fig. 5, 6** are Scanning Electron Microscope (SEM) images of the coating with porosity analysis at 500x magnification.

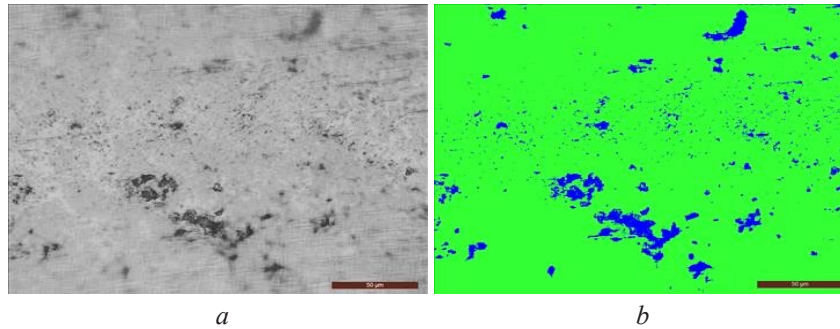


Fig. 5. Magnified image $\times 500$ coating contains porosity: a – the original image; b – the processed image

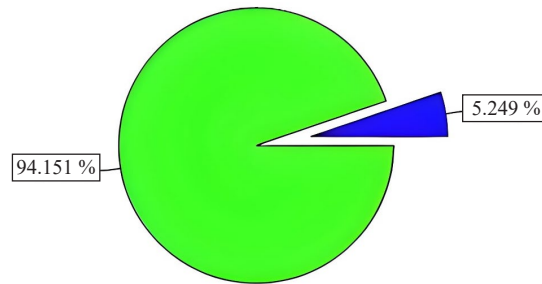


Fig. 6. Analysis image in % of coating porosity

With three input parameters F , D , and R , using the Taguchi L9 orthogonal table with the coating porosity measurement results as in **Table 4**.

To analyze the influence of F , D , and R on Po , use the SN_i factor [8]:

$$SN_i = -10 \log \left(\frac{\sum_{u=1}^{N_i} y_u^2}{N_i} \right) \quad (1)$$

In which $i = 1-9$; u – test times ($u = 1-3$); N_i – number of trials for experiment i ($N_i = 3$).

So SN_i factors are shown in **Table 5**.

Table 4

Coating porosity measurement results according to Taguchi L9 table

| No. | F (g/min) | D (m) | R | Po (%) (1 st) | Po (%) (2 nd) | Po (%) (3 rd) | \overline{Po} (%) |
|-----|-------------|---------|-----|-----------------------------|-----------------------------|-----------------------------|---------------------|
| 1 | 25 | 0.2 | 4 | 5.249 | 5.152 | 5.373 | 5.258 |
| 2 | 25 | 0.25 | 5 | 4.973 | 4.863 | 4.845 | 4.894 |
| 3 | 25 | 0.3 | 6 | 3.228 | 3.348 | 3.148 | 3.241 |
| 4 | 30 | 0.2 | 5 | 5.059 | 4.943 | 4.875 | 4.959 |
| 5 | 30 | 0.25 | 6 | 3.086 | 3.294 | 3.102 | 3.161 |
| 6 | 30 | 0.3 | 4 | 3.986 | 4.034 | 3.883 | 3.968 |
| 7 | 35 | 0.2 | 6 | 4.688 | 4.832 | 4.593 | 4.704 |
| 8 | 35 | 0.25 | 4 | 3.767 | 3.912 | 3.871 | 3.850 |
| 9 | 35 | 0.3 | 5 | 3.109 | 3.135 | 3.285 | 3.176 |

Table 5
The SN_i factors are calculated for coating porosity

| No. | F (g/min) | D (m) | R | Po |
|-----|-------------|---------|-----|----------|
| | | | | SN_i |
| 1 | 25 | 0.2 | 4 | -14.4177 |
| 2 | 25 | 0.25 | 5 | -13.7933 |
| 3 | 25 | 0.3 | 6 | -10.2173 |
| 4 | 30 | 0.2 | 5 | -13.9089 |
| 5 | 30 | 0.25 | 6 | -9.99946 |
| 6 | 30 | 0.3 | 4 | -11.9718 |
| 7 | 35 | 0.2 | 6 | -13.4519 |
| 8 | 35 | 0.25 | 4 | -11.7103 |
| 9 | 35 | 0.3 | 5 | -10.0411 |

The SN factor is calculated for each indicator and level as follows:

$$SN_{P1,1} = \frac{(SN_1 + SN_2 + SN_3)}{3}, SN_{P1,2} = \frac{(SN_4 + SN_5 + SN_6)}{3},$$

$$SN_{P1,3} = \frac{(SN_7 + SN_8 + SN_9)}{3}, SN_{P2,1} = \frac{(SN_1 + SN_4 + SN_7)}{3},$$

$$SN_{P2,2} = \frac{(SN_2 + SN_5 + SN_8)}{3}, SN_{P2,3} = \frac{(SN_3 + SN_6 + SN_9)}{3},$$

$$SN_{P3,1} = \frac{(SN_1 + SN_6 + SN_8)}{3}, SN_{P3,2} = \frac{(SN_2 + SN_4 + SN_9)}{3},$$

$$SN_{P3,3} = \frac{(SN_3 + SN_5 + SN_7)}{3}.$$

The SN values for each parameter are presented in **Table 6**.

Table 6
Signal factors (SN) showing the degree of influence of experimental parameters on coating porosity

| Level | Po | | |
|-------|-------------------------|-------------------------|-------------------------|
| | SN calculated for F | SN calculated for D | SN calculated for R |
| 1 | -12.8094 | -13.9262 | -2.6999 |
| 2 | -11.9601 | -11.8343 | -2.5811 |
| 3 | -11.7344 | -10.7434 | -1.2229 |
| R | 1.0750 | 3.1828 | 1.4771 |

The results in **Table 6** show that the spray distance has the greatest influence on the coating porosity, following by the oxygen/propane ratio and the spray flow has the least influence on the three parameters.

Using ANOVA analysis [9, 10] to evaluate the influence of each main parameter (F , D , R) and interactive effects of parameters on the coating porosity, the results were obtained and presented in **Fig. 7, 8**.

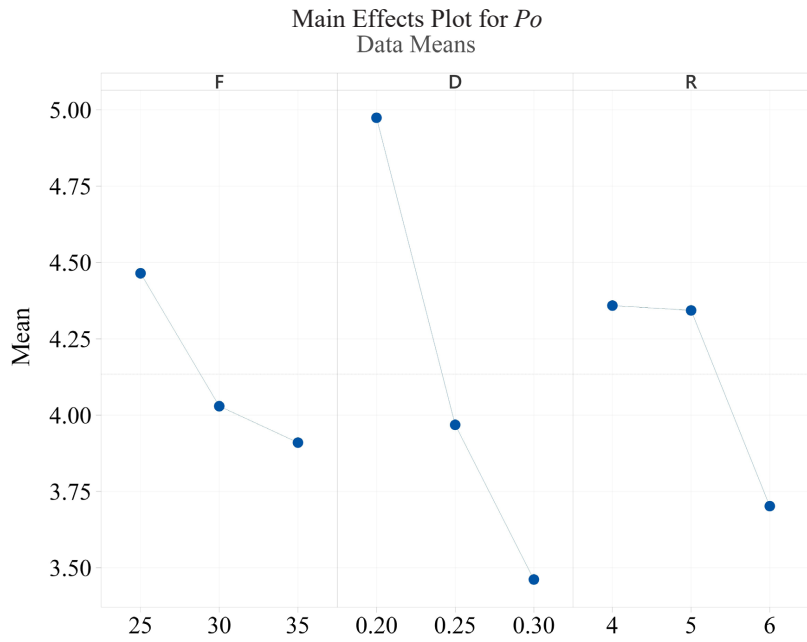


Fig. 7. Graph of the influence of each main parameter on coating porosity

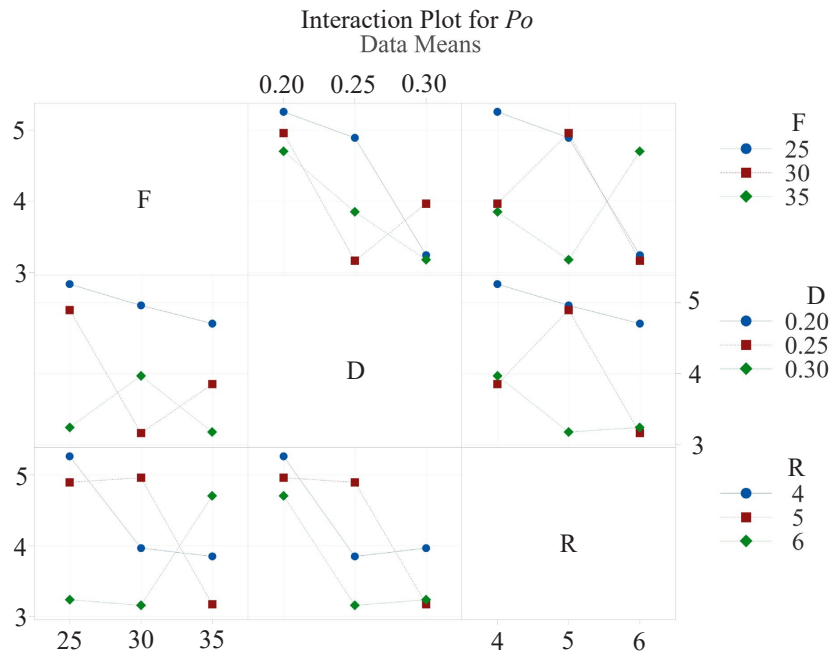


Fig. 8. Graph of interactive effects of parameters on coating porosity

(2) displays the empirical regression equation that illustrates the correlation between spray mode parameters and coating porosity:

$$Po = -0.4813F + 49.57D + 3.717R + 0.009371F^2 + 29.24D^2 - 0.5647R^2 - 2.016F*D + 0.07049F*R - 3.058D*R. \quad (2)$$

From the graphs presented in Fig. 7, 8, as well as (2), it is evident that the appropriate spray mode for achieving the lowest porosity is $F_3D_3R_3$, where F denotes a spray rate of 35 g/min, D represents a spray distance of 0.3 m, and R signifies an oxygen/propane ratio of 6. Furthermore,

the degree of interaction between D and R , as well as between F and D , is significant, whereas the interaction between F and R is relatively low.

3. 2. Analysis results of coating hardness

Taguchi L9 orthogonal table with coating hardness measurement results (H) is shown in Table 7.

Table 7

Coating hardness measurement results according to Taguchi L9 Table

| No. | F (g/min) | D (m) | R | H (HRC) (1 st) | H (HRC) (2 nd) | H (HRC) (3 rd) | \bar{H} (HRC) |
|-----|-------------|---------|-----|------------------------------|------------------------------|------------------------------|-----------------|
| 1 | 25 | 0.2 | 4 | 70.51 | 71.07 | 70.92 | 70.83 |
| 2 | 25 | 0.25 | 5 | 75.76 | 74.70 | 73.96 | 74.81 |
| 3 | 25 | 0.3 | 6 | 70.03 | 69.29 | 69.12 | 69.48 |
| 4 | 30 | 0.2 | 5 | 71.30 | 70.66 | 69.72 | 70.56 |
| 5 | 30 | 0.25 | 6 | 72.45 | 71.87 | 72.98 | 72.43 |
| 6 | 30 | 0.3 | 4 | 76.44 | 75.85 | 75.19 | 75.83 |
| 7 | 35 | 0.2 | 6 | 70.78 | 71.21 | 71.73 | 71.24 |
| 8 | 35 | 0.25 | 4 | 78.67 | 79.3 | 76.50 | 78.16 |
| 9 | 35 | 0.3 | 5 | 71.57 | 70.22 | 71.28 | 71.02 |

The SN_i factors are calculated for coating hardness shown in Table 8.

Table 8

The SN_i factors are calculated for coating hardness

| No. | F (g/min) | D (m) | R | H SN_i |
|-----|-------------|------------|-----|---------------|
| 1 | 25 | 0.2 | 4 | -37.0048 |
| 2 | 25 | 0.25 | 5 | -37.4792 |
| 3 | 25 | 0.3 | 6 | -36.8373 |
| 4 | 30 | 0.2 | 5 | -36.9715 |
| 5 | 30 | 0.25 | 6 | -37.1989 |
| 6 | 30 | 0.3 | 4 | -37.5966 |
| 7 | 35 | 0.2 | 6 | -37.0546 |
| 8 | 35 | 0.25 | 4 | -37.8603 |
| 9 | 35 | 0.3 | 5 | -37.0283 |

The SN values for each parameter are presented in Table 9.

Table 9

Signal factors (SN) showing the degree of influence of experimental parameters on coating hardness

| Level | Po | | |
|-------|-------------------------|-------------------------|-------------------------|
| | SN calculated for F | SN calculated for D | SN calculated for R |
| 1 | -37.10712 | -37.0103 | -37.4873 |
| 2 | -37.2557 | -37.5128 | -37.1597 |
| 3 | -37.31442 | -37.1541 | -37.0303 |
| R | 0.2073 | 0.5025 | 0.4570 |

Upon examining the results displayed in **Table 9**, it can be concluded that the spray distance exerts the most substantial impact on the coating hardness, following the spray distance, the oxygen/propane ratio is the second most influential factor, while the spray flow exhibits the least effect on the three parameters. It is worth noting that the degree of influence of each factor does not differ significantly.

Using ANOVA analysis to evaluate the influence of each main parameter (F , D , R) and interactive effects of parameters on the coating hardness, the results were obtained and presented in **Fig. 9, 10**.

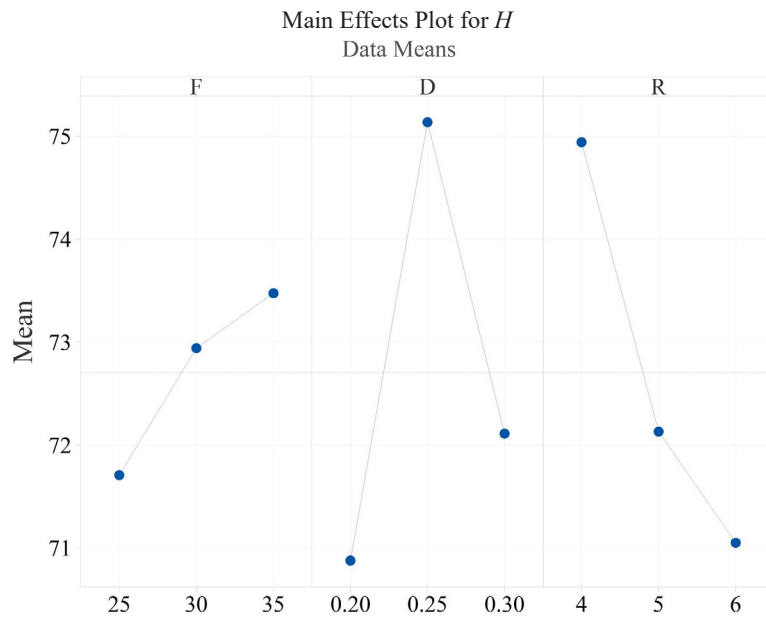


Fig. 9. Graph of the influence of each main parameter on coating hardness

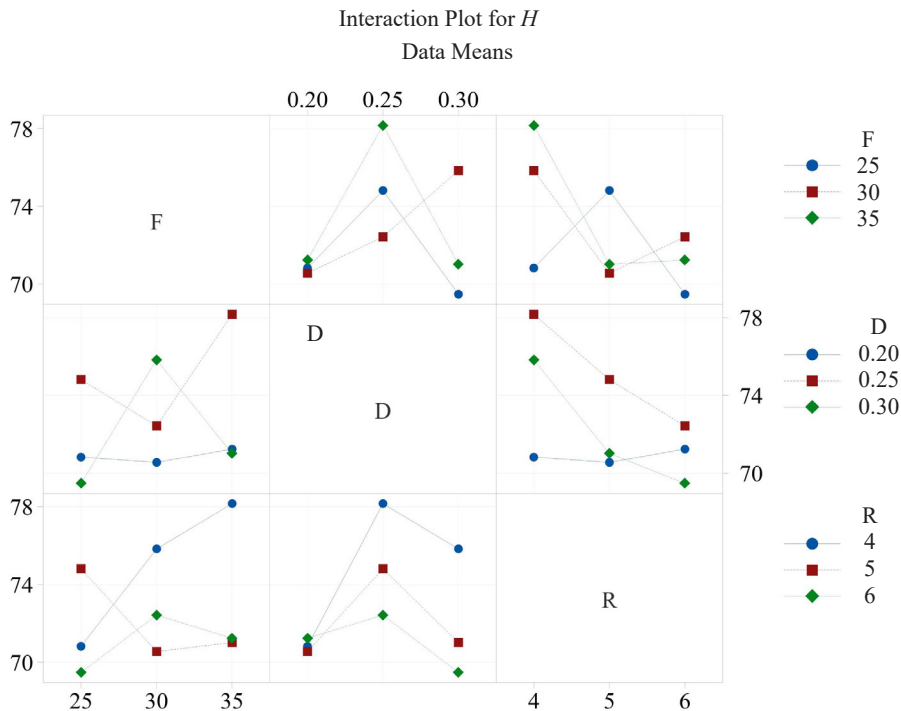


Fig. 10. Graph of interactive effects of parameters on coating hardness

(3) illustrates the experimental regression equation that depicts the correlation between spray mode parameters and coating hardness:

$$H = -87.52 + 2.323F + 1179D - 6.555R - 0.01400F^2 - 1701D^2 - 0.4017R^2 - 10.13F*D + 0.2453F*R. \quad (3)$$

Upon examining the graphs presented in **Fig. 9, 10**, as well as (3), it can be deduced that the appropriate spray mode for achieving the highest coating hardness is $F_3D_2R_3$, where F denotes a spray rate of 35 g/min, D represents a spray distance of 0.25 m, and R signifies an oxygen/propane ratio of 6. Additionally, the degree of interaction between F and D is substantial, while the interaction between F and R is relatively low. It is also noteworthy that there is no interaction between F and R .

4. Conclusions

In this study, the influence of spray parameters, including spray flow, spray distance, and oxygen/propane ratio, on the structure and hardness of WC HMSP1060-00+60 % 4070 coating on the surface of a pressing screw made of 1045 steel, was investigated and analyzed. The results indicated that the spray distance had the most significant impact on the coating hardness, following by the oxygen/propane ratio and the spray flow rate. Although the spray distance exhibited the greatest influence on coating hardness, the impact of spray distance, oxygen/propane ratio, and spray flow was not substantially different. A spray flow value of $F = 35$ g/min and an oxygen/propane ratio of $R = 6$ were found to be suitable for achieving low porosity and high stiffness. Moreover, the spray distance value needed to be adjusted between 0.25 m to 0.3 m to balance porosity and hardness. These analyses could aid in selecting the appropriate injection mode to improve the pressing screw's performance under high loads and abrasion by achieving low porosity and high hardness. However, in addition to evaluating the hardness and porosity of the coating, to achieve even higher quality, further research is needed on other factors of the coating such as adhesion or abrasion, ability to heat resistant.

Conflict of interest

The authors declare that they have no conflict of interest in relation to this research, whether financial, personal, authorship or otherwise, that could affect the research and its results presented in this paper.

Financing

The study was performed without financial support.

Data availability

Manuscript has no associated data.

Use of artificial intelligence

The authors confirm that they did not use artificial intelligence technologies when creating the current work.

References

- [1] Tapphorn, R. M., Gabel, H. (1998). The solid-state spray forming of low-oxide titanium components. *JOM*, 50 (9), 45–47. doi: <https://doi.org/10.1007/s11837-998-0414-3>
- [2] Davis, J. R. (Ed.) (2004). *Thermal Spray Processes*. Thermal Spray Technology. ASM International. Available at: <https://studylib.net/doc/27015902/davis-j.r.-handbook-of-thermal-spray-technology--asm-i>
- [3] *HVOF Thermal Spray Deposition Of Functionally Graded Coatings* (2005). Dublin City University.
- [4] Poirier, D., Legoux, J.-G., Lima, R. S. (2012). Engineering HVOF-Sprayed Cr3C2-NiCr Coatings: The Effect of Particle Morphology and Spraying Parameters on the Microstructure, Properties, and High Temperature Wear Performance. *Journal of Thermal Spray Technology*, 22 (2-3), 280–289. doi: <https://doi.org/10.1007/s11666-012-9833-3>

- [5] Pawlowski, L. (2008). *The Science and Engineering of Thermal Spray Coatings*. John Wiley & Sons. doi: <https://doi.org/10.1002/9780470754085>
- [6] Bringas, J. E. (Ed.) (2004). *Handbook of comparative world steel standards*. ASTM DS67B.
- [7] ASTM E384-17. *Standard Test Method for Microindentation Hardness of Materials*. Available at: <https://cdn.standards.iteh.ai/samples/97981/e209001124704a8da2631f46a036ac64/ASTM-E384-17.pdf>
- [8] Roy, R. K. (2001). *Design of Experiments Using the Taguchi Approach: 16 Steps to Product and Process Improvement*. John Wiley & Sons.
- [9] Montgomery, D. C. (2019). *Design and Analysis of Experiments*. John Wiley & Sons, 688.
- [10] Arora, J. S. (2012). *Introduction to Optimum Design*. Elsevier. doi: <https://doi.org/10.1016/c2009-0-61700-1>

Received date 06.06.2023

Accepted date 15.11.2023

Published date 30.11.2023

© The Author(s) 2023

This is an open access article

under the Creative Commons CC BY license

How to cite: *Nguyen, T.-L., Nguyen, H. T., Nguyen, V. T., Khuat, D. D. (2023). Analysis of the effect of spray mode on coating porosity and hardness when spraying press screws by the high velocity oxy fuel method. EUREKA: Physics and Engineering, 6, 93–103. doi: <https://doi.org/10.21303/2461-4262.2023.003161>*